A nanoporous optically transparent CdS–pHEMA hybrid with high optical sensing capability to dielectric liquids

2009 Nanotechnology 20 095504

(http://iopscience.iop.org/0957-4484/20/9/095504)

Nanotechnology **20** (2009) 095504 (8pp) doi:10.1088/0957-4484/20/9/095504

A nanoporous optically transparent CdS–pHEMA hybrid with high optical sensing capability to dielectric liquids

Hung-Chou Liao, Yen-Yu Liu, San-Yuan Chen[1] and Dean-Mo Liu[1]

Department of Materials Science and Engineering, National Chiao Tung University, 1001 Ta-Hsueh Road, Hsinchu, 30010 Taiwan, Republic of China

E-mail: sanyuanchen@mail.nctu.edu.tw and deanmo_liu@yahoo.ca

Received 15 October 2008, in final form 28 November 2008
Published 11 February 2009
Online at stacks.iop.org/Nano/20/095504

Abstract

A hydrogel-based functional hybrid with highly uniformly dispersed nanoparticulate CdS semiconductors is proposed. The hybrid is synthesized using an *in situ* polymerization following an *in situ* chemical reduction, where the resulting particle size and the distribution of CdS nanocrystals (NCs) can be narrowly manipulated. The hybrids, containing a relatively small amount of the CdS NCs, exhibit a pronounced photoluminescence spectrum shift when in contact with a number of dielectric liquids and such a pronounced dielectric-confinement effect has been experimentally verified and modeled in this study. The sensing capability of the hybrids with respect to dielectric liquids or molecules can be optically characterized and varied depending upon the intensity of the dielectric environment surrounding the hybrids. This work suggests that the transparent, nanoporous CdS–pHEMA hybrids can be used as highly efficient optical sensing materials.

(Some figures in this article are in colour only in the electronic version)

1. Introduction

Recently, exploring novel materials based on quantum dots, i.e. semiconductor nanocrystals (NCs), have attracted enormous attention worldwide [1–3]. The great interest in colloidal semiconductor NCs derived from their unique luminescence properties, i.e. a consequence of quantum-confinement effects, gives rise to their potential use in a variety of fields, for example, light-emitting diodes [4, 5], biolabeling [6–8], sensors [9, 10] and photonic crystals [11]. Moreover, CdS NCs are representative examples of group II–VI semiconductor NCs with strong photoluminescence emission which could be synthesized in aqueous solution with simplicity and high reproducibility.

In order to take full advantage of the semiconductor NCs with superior unique luminescence properties in practical applications, it is necessary that the inherently unstable particles are stabilized using inert inorganic or organic matrices. For instance, enclosing semiconductor NCs in polymer matrices is an effective method of enhancing the functionality of these materials [12]. Many research groups have focused on the superior emitting properties of nanocomposites by dispersing the quantum dots into a polymeric matrix [13–17]. These nanocomposites not only inherit the high luminescence of the quantum dots but also possess the advantages of polymers such as flexibility, film integrity and conformity. The proper management of the particle size, size distribution and dispersion homogeneity of the quantum dots over the entire matrix is the critical prerequisite to ensure the best performance of the optical properties of the nanocomposites for technical applications.

Up to now, to employ a polymer as a solid matrix for the physical immobilization of inorganic NCs is still a technological challenge [18, 19] because few approaches have attempted to prepare nonaggregated NCs in a transparent polymer matrix. Generally, modifying NCs surface with appropriate ligands such as long chain aliphatic thiols [20, 21] or amines [22] is the most powerful and widely used method to prevent aggregation of the innately unstable NCs and thus enhance both the physical and chemical compatibilities of the inorganic NCs with the organic matrix. In addition, fewer

[1] Authors to whom any correspondence should be addressed.

studies [12, 23–27] also showed that *in situ* synthesis of inorganic NCs in a polymer matrix is possible and attractive. However, the application and relevant technical performance of these nanocomposites has been hindered by the fact that the inorganic NCs cannot be distributed highly uniformly within the polymeric matrices.

In order to overcome this problem, we employed an *in situ* water-based forming technique using selected ionic precursors, rendering the resulting CdS NCs which can be easily synthesized in aqueous solution. Accordingly, 2-hydroxyethyl methacrylate (HEMA) monomers are hydrophilic, and its polymerized form, namely poly(HEMA), has been well known as a mechanically strong and flexible, optically transparent polymeric material, and the positively charged Cd^{2+} ions can be chemically anchored or chelated by the unpaired electron of O from the COOR group of the HEMA monomers, so we employ HEMA monomers and Cd^{2+} precursors to prepare CdS–pHEMA hybrids. The *in situ* method is able to produce a novel hybrid nanocomposite system with highly well-dispersed CdS NCs embedded in a pHEMA hydrogel matrix by an *in situ* CdS synthesis following an *in situ* photopolymerization. What is more technically interesting is that the CdS quantum dots can be dispersed in the hydrogel in nanometric uniformity. Furthermore, such a well-dispersed hybrid system, once being technically achieved, can be designed as having the combined advantages of enhanced photoluminescent behavior of the CdS NCs associated with the transparent, flexible, and nanoporous pHEMA matrix for a number of technological applications, such as a chemical sensor with high sensitivity to a subtle variation of its environment. In this investigation, we reported that CdS NCs in the hydrogel matrix showed an exceptional photoluminescence behavior while contacting dielectric liquids, where the photoluminescence behavior and the mechanism behind it are discussed.

2. Experimental details

2.1. Materials

The hydrogel matrix was synthesized using 2-hydroxyethyl methacrylate (HEMA, Sigma-Aldrich, Inc. USA, analytical grade) monomer and ethylene glycol dimethacrylate (EGDMA, Sigma-Aldrich, Inc. USA, analytical grade) as a cross-linker, and benzoin methyl ether (BME, Tokyo Chemical Industry, analytic grade). $Cd(NO_3)_2$ (Sigma-Aldrich, Inc. USA, analytic grade) was employed as the precursor for CdS formation and Na_2S (Sigma-Aldrich, Inc. USA, analytical grade) was used as the reducing agent for *in situ* CdS NCs formation.

2.2. CdS–pHEMA hybrid synthesis

The CdS–pHEMA hybrid was prepared by employing UV irradiation on an aqueous solution containing 3 g of HEMA monomer, 0.12 ml of EDGMA as cross-linker, 0.3 g BME as initiator and 1 ml Cd^{2+} solution. The Cd(II)–pHEMA hybrid was rinsed by distilled water to remove the unreacted species (e.g. cross-linker, monomer, etc) and then subjected to *in situ* chemical reduction by immersion of the as-synthesized Cd^{2+}–pHEMA hybrid into 100 ml of Na_2S for 24 h to form the final CdS–pHEMA hybrid.

2.3. Structural and optical properties analysis

To investigate the nanostructure of the CdS–pHEMA hybrid, transmission electron microscopy (TEM; JEOL, JEM-2100F, field emission transmission electron microscope) was employed. For TEM images, the particle size and particle distribution of the resulting CdS in the hybrid can be examined. The resulting hybrid was sliced using a Leica EM UC6 Ultramicrotome with EMFCS cryoattachment at room temperature. The cross sections of approximately 100 nm in thickness were obtained by using a diamond knife. The ultrathin films of the hybrid were directly placed on the copper grids. TEM micrographs were acquired at an operating voltage of 200 kV. The crystal structure of the CdS–pHEMA hybrid was determined by x-ray diffraction with Cu Kα radiation and an Ni filter (Siemens D5000). Optical properties are analyzed by UV–vis spectroscopy and photoluminescence spectrometer (Hitchai F4500) equipped with an excitation source of 450 nm wavelength. The measurements were done in standard humidity atmospheres by the use of saturated salt solutions at 25 °C in a closed system. The relative humidity values used were: 11% (LiC1), 33% ($MgC1_2{\cdot}6H_2O$), 43% (K_2CO_3) and 81% ($(NH_4)_2SO_4$) [28]. The samples were preconditioned at the appropriate relative humidity for 48 h before testing.

3. Results and discussion

3.1. Structure development

Figures 1(a) and (b) illustrate the appearance of the CdS–pHEMA hybrids prepared using different starting cadmium concentrations under visible light and UV exposure, respectively. The resulting hybrids show a transparent appearance in the visible region. However, they display different colors in the UV region, suggesting a nanostructural variation of the CdS NCs upon synthesis. No phase separation between the CdS NCs and pHEMA in the hybrid was experimentally observed, indicating both phases are compatibly well distributed during the course of the synthesis and the nanophasic CdS is likely to be well localized or immobilized within the network structure of the pHEMA matrix. The x-ray diffraction (XRD) pattern of the hybrid (not shown here) indicated a typical cubic zinc blende crystalline structure which is in agreement with that of the standard XRD of crystalline CdS (JCPDS card no. 10-454), indicating the nanophasic NCs are CdS nanoparticles.

Figure 2(a) shows the TEM image of one of the CdS–pHEMA hybrids, prepared using 1.0 M Cd^{2+} concentration, which confirms that the nanophasic CdS NCs having a relatively uniform size of 4–5 nm in diameter (inset photo) are highly uniformly dispersed within the pHEMA matrix. However, some nanocrystals, derived from higher Cd^{2+} concentrations such as 3.0 M, showed a sparingly distributed,

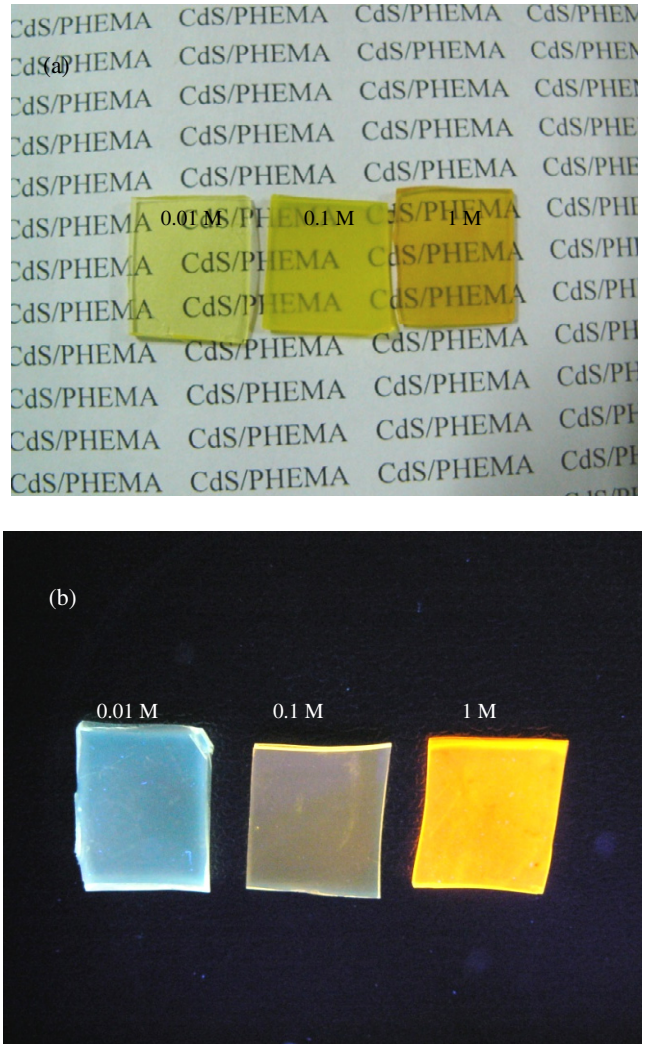

Figure 1. (a) A photograph of CdS–pHEMA hydrogels with various Cd^{2+} concentrations under sunlight, showing its transparent and homogeneous properties. (b) A photograph of three different CdS–pHEMA hydrogels excited by an ultraviolet lamp. The average diameters of the CdS NC are estimated to be 3.2 nm (left), 3.8 nm (middle) and 4.4 nm (right).

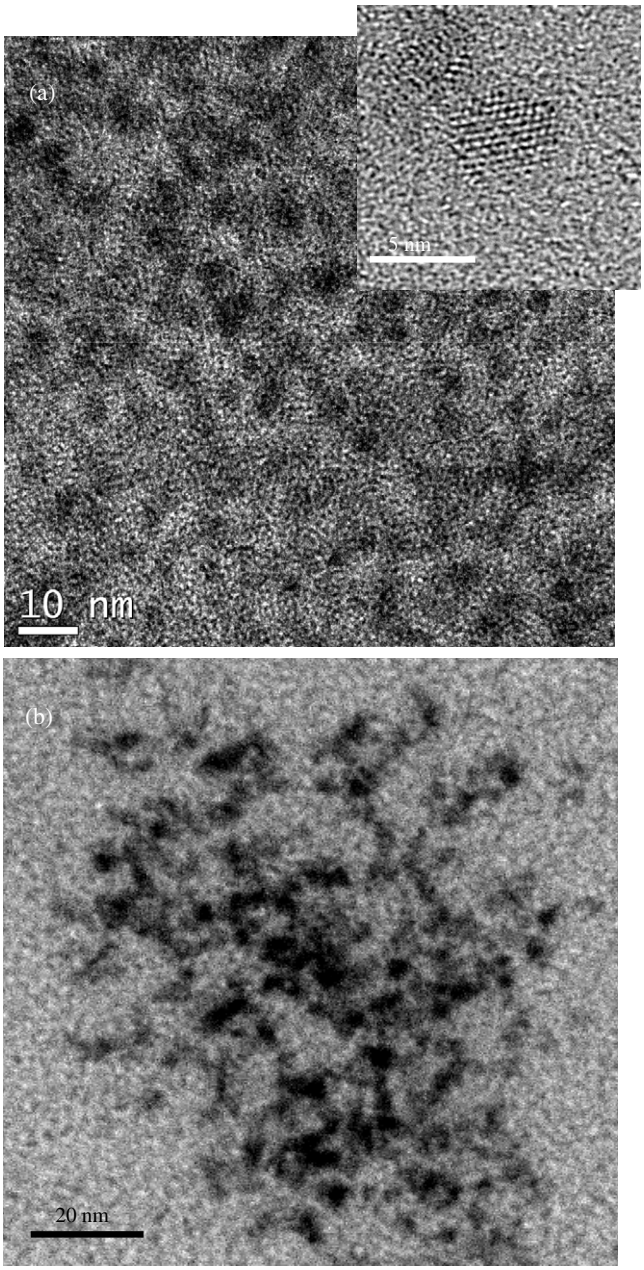

Figure 2. (a) A TEM image of CdS–pHEMA hybrid synthesized using 1.0 M Cd^{2+} concentration by the *in situ* method. The nanoparticles are highly uniformly dispersed within the pHEMA matrix, with the inset showing a high resolution TEM image of CdS NCs. (b) CdS–pHEMA hybrid with a higher Cd^{+2} concentration of 3 M, showing a sparingly fractal nanostructure intertwined with the pHEMA matrix.

short-range, i.e. of the order of 50–100 nm in dimension, fractal nanostructure intertwined with the pHEMA matrix, as shown in figure 2(b). The nanophasic CdS NCs can also be clearly distinguished which have an average size of 4.5 ± 0.6 nm in diameter. The size of the resulting CdS NCs was found to increase with the starting Cd concentration upon synthesis.

Since the light-emitting character of the CdS quantum dots is size-dependent [29], the dimensions of the CdS NCs were further characterized by UV–vis spectroscopy. The position of the absorption edge (λ_e), for lower starting Cd^{2+} concentrations of 0.01 M, 0.1 M and 1 M is at 437, 458 and 474 nm, respectively, which, through the use of equation (1), the corresponding diameter (R_{CdS}) of the CdS nanoparticle was estimated to be approx. 3.2 nm, 3.8 nm and 4.4 nm for the hybrids, respectively [30, 31]:

$$R_{CdS} = 0.1/(0.1338 - 0.000\,2345\lambda_e). \quad (1)$$

The particle size of the CdS NCs calculated from the spectrum is relatively close to that microscopically observed, i.e. figure 2(a), which further substantiates the NCs experimentally observed are virtually displaying a primary particle, without the formation of appreciable secondary structure upon hybrid synthesis, and it is most pronounced for those derived from low Cd^{2+} concentrations. Apparently, the size of the CdS NCs is linearly proportional to the logarithmic value of the Cd^{2+} concentration, suggesting a logarithmic-dependent growth behavior of the NCs with respect to the

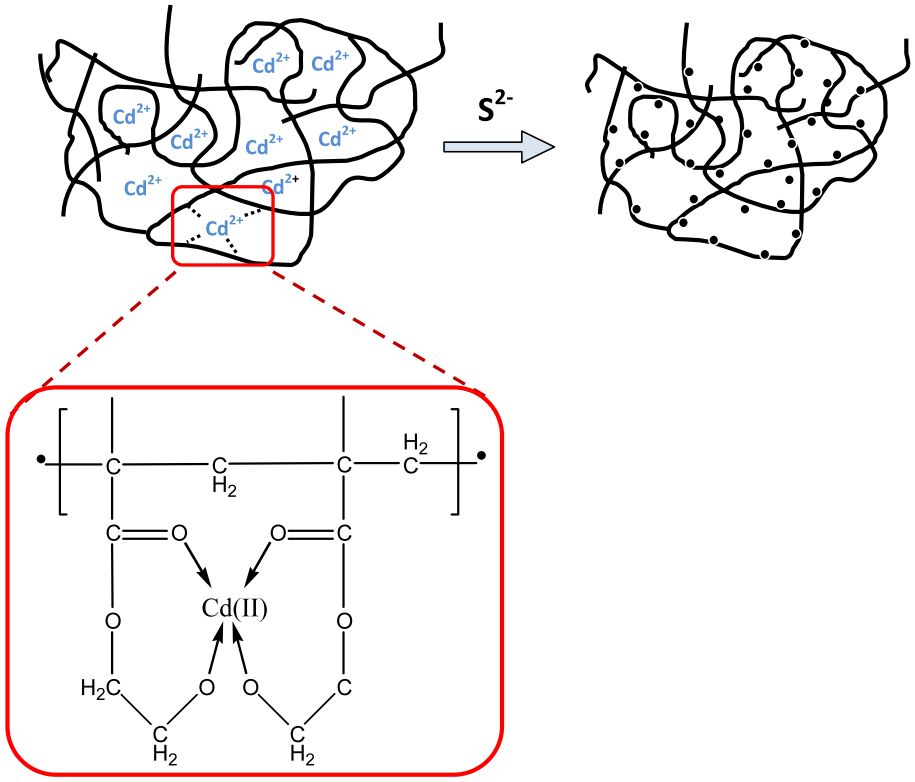

Figure 3. Schematic drawing for the proposed synthesis scheme of CdS–pHEMA hybrids. The Cd^{2+} ions were assumed to be coupled with the unpaired O of COOR groups along the pHEMA chain network, and the Cd^{2+} ions were localized and chemically reduced by Na_2S *in situ* to CdS NCs. (●) indicates CdS NCs synthesized in hybrids.

Cd precursor concentration. Upon hybrid synthesis, as has been reported elsewhere [32], we believed that the Cd^{2+} ions can be anchored or chelated by the unpaired electron of O from the COOR group of the HEMA monomers in the starting mixture, forming a chemical complex, as schematically illustrated in figure 3. The Cd^{2+} ions are then immobilized in a confined space within the network structure of the pHEMA upon polymerization and stayed in place while being subjecting to a subsequent nucleation-and-growth process with sulfur ions, resulting in highly uniformly distributed CdS NCs in the matrix, as shown in figure 2(a). However, when the Cd^{2+} concentration increased, e.g. 3 M, free Cd^{2+} ions, i.e. the extra ones that are not anchored to the unpaired electron O due to the unavailability of the unpaired electron oxygen for a given amount of HEMA, led to an unexpectedly exaggerated development of the CdS NCs composed of larger CdS NCs together with the presence of a short-range ordered fractal network. Such a size variation, about 17–18%, albeit not significant, gives rise to a pronounced variation in color appearance in the resulting hybrid. Figure 4 shows the photoluminescence spectra of the water-saturated CdS–pHEMA hybrids with different starting Cd^{2+} ion concentrations under an excitation wavelength at 450 nm. The maximum wavelengths of the emission band of CdS–pHEMA hybrids were blueshifted from 618 to 508 nm when the Cd^{2+} ion concentration was decreased by two orders of magnitude from 1.0 to 0.01 M. The emission band is attributed to the recombination of charge carriers of surface defect states [31] and the blueshift of the emission peak is due

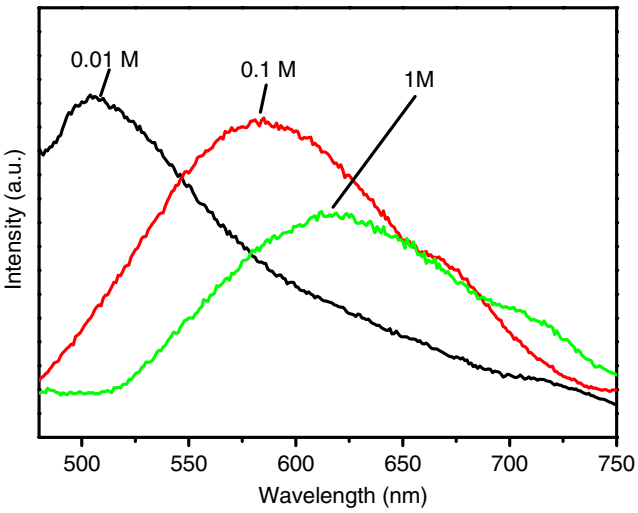

Figure 4. Photoluminescence emission spectra of water-saturated CdS–pHEMA hybrids with various Cd^{2+} concentrations.

to the size effect of the CdS NCs [29]. This finding clearly indicates a size-specific variation in the band energy structure and has been elucidated in a number of reports [29, 33].

3.2. Photoluminescence emission of the hybrid

pHEMA is a mechanically strong hydrogel capable of absorbing and retaining relatively high amounts of water

molecules within the network structure, and has long been used for contact lenses. In order to keep the swollen structure of the hybrid, the water-swollen hybrid was freeze-dried in vacuum, and then characterized using BET analysis, where a specific surface area as large as 186 $m^2\ g^{-1}$ was measured, indicating a nanoporous hybrid with an average pore size in the region of a few nanometers. Therefore, a combination of the highly dispersed CdS NCs, i.e. the one prepared using 1.0 M Cd precursor, and nanoporous pHEMA hydrogel is expected to allow the largest surface area of the encapsulated CdS NCs to be exposed to and interact with a given environmental stimulus. Once this proves to be technically feasible, it is postulated that the largest exposure of the CdS NCs, even in a lower concentration, within the nanoporous matrix will give rise to a stronger accumulative response (or sensitivity) compared to those with a certain degree of agglomeration, giving rise to a change in its light emission behavior.

To confirm this argument, we first exposed the resulting hybrid (containing ∼10 wt%, corresponding to about 4 vol%, of CdS NCs) to water, having a dielectric constant ∼81, under a controllable manner as illustrated in figure 5(a), where the photoluminescence emission spectra of the CdS–pHEMA hybrid were changed considerably with varying degrees of relative humidity (RH) ranging from 0% (prepared under a freeze-dried condition) to 81% and considered as 100% for the water-saturated hybrid, i.e. under a water-swollen condition. The wavelength of the corresponding photoluminescence emission peaks decreased with decreasing RH, where, for the 100% RH sample, it shows a maximum at 618 nm, and for the 0% RH sample a considerable blueshift to 547 nm was detected. Plotting the photoluminescence spectrum shift with respect to the value of RH, from 0% to 81%, gives a relationship as illustrated in figure 5(b), where the spectrum shift appears to increase in a polynomial manner relative to the value of relative humidity over the range of 0%–81%. A blueshift of the spectrum by as large as 71 nm was observed between 0% and 100% RH, indicating a strong emission response of the highly dispersed CdS NCs relative to their microenvironmental change. In other words, the CdS NCs with a considerably large surface area were being exposed to water molecules and this should alter the optical characteristics of the CdS NCs within the nanoporous hybrid.

This spectral variation may be referred to as a dielectric-confinement effect [34, 35], which is originally induced by the local field correction of a doped particle in contact with a dielectric medium. It is well known that quantum confinement enhances the allowed energies, resulting in an increase in binding energy of shallow impurities. The static dielectric constant both in the quantum dots and their matrix could be contributing to the binding energy of a donor or an acceptor via dielectric screening and the effect on induced charges at the dielectric interface. A computational simulation of a quantum dot system has been put forward by Tsu and Babic [34], who showed that an increase of the dielectric constant of the matrix should cause a decrease of the binding energy.

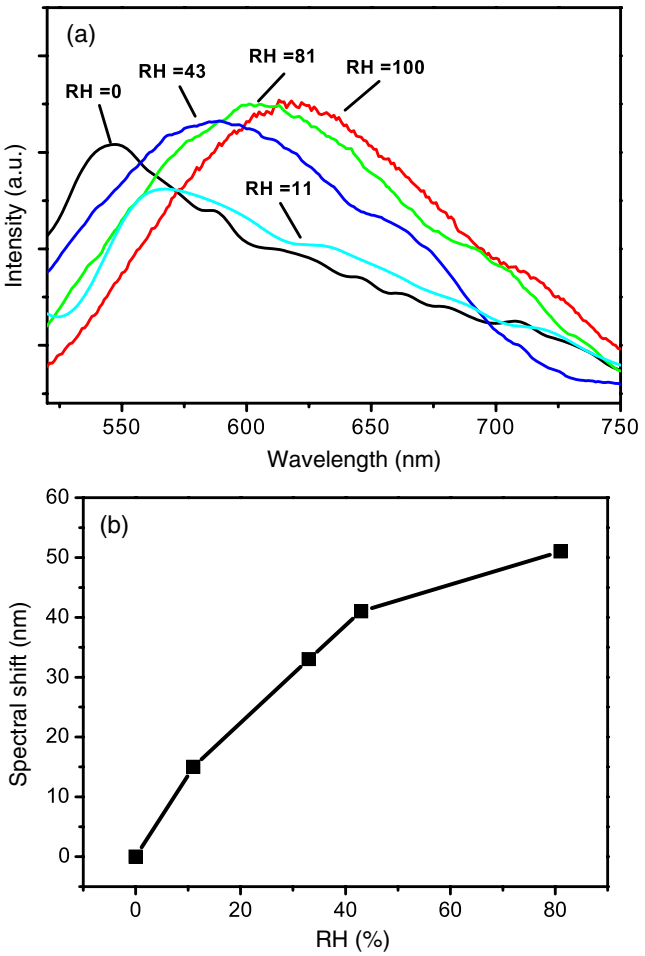

Figure 5. (a) Photoluminescence emission spectra of CdS–pHEMA hybrids with different RH. (b) Relationship between the shift of emission peak and RH.

3.3. Dielectric-induced photoluminescence spectrum shift

To further prove this concept, freeze-dried CdS–pHEMA hybrids were employed and exposed to a number of dielectric solvents for 24 h, in order to ensure full saturation of the hybrid with the dielectric liquids, which included 2-pentanol ($\varepsilon = 18$), ethanol ($\varepsilon = 25$), ethylene glycol ($\varepsilon = 38$), glycerol ($\varepsilon = 45$), 40% water + 60% ethylene glycol ($\varepsilon = 61$), 70% water + 30% ethylene glycol ($\varepsilon = 72$) [36], together with water ($\varepsilon = 81$), and is representing a 100% saturation (swollen by solvent), followed by photoluminescence emission measurement, as illustrated in figure 6(a). The wavelength of the corresponding photoluminescence emission peaks increased with increasing the dielectric constant of liquids, compared with the freeze-dried sample. For the hybrid equilibrated with the dielectric liquids, the hybrid was indeed undergoing no appreciable change in structural integrity whereas the nanoporous structure of the hybrid remained identical. An effective dielectric constant as a result of the combination of pHEMA and solvents has to be estimated. Therefore, based on Gao's model [37], the effective dielectric constant (ε_{eff}) can be

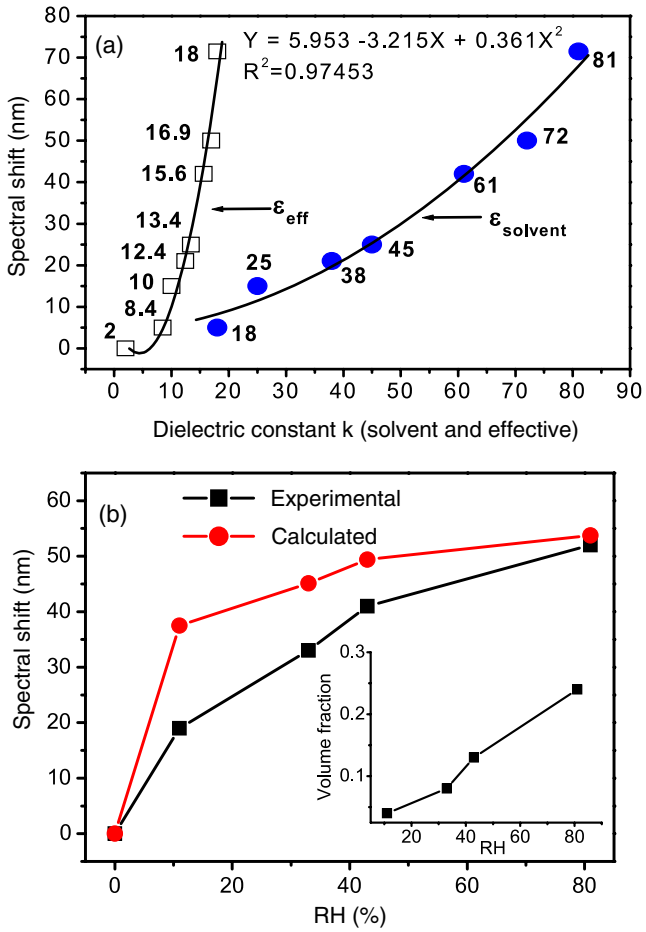

Figure 6. (a) Photoluminescence spectrum shift versus (effective) dielectric constant of solvent. (b) Experimental and calculated spectrum shift versus RH. Inset: RH versus volume fraction of water.

reasonably approximated as

$$\varepsilon_{\text{eff}} = \varepsilon_{\text{pHEMA}}\left[\frac{1 + f(\sqrt{\varepsilon_{\text{solvent}}/\varepsilon_{\text{pHEMA}}} - 1)}{1 + f\sqrt{\varepsilon_{\text{pHEMA}}/\varepsilon_{\text{solvent}}} - 1}\right] \quad (2)$$

where ε is the dielectric constant and f is the volume fraction of the solvent.

The volume fraction of the CdS NCs in the hybrid is relatively small, about 4 vol%. After rearrangement of equation (2) and incorporating the value of $\varepsilon_{\text{pHEMA}} = 4$, ε_{eff} can be expressed as

$$\varepsilon_{\text{eff}} = 4\left[\frac{1 + f(\sqrt{\varepsilon_{\text{solvent}}/4} - 1)}{1 + f\sqrt{4/\varepsilon_{\text{solvent}}} - 1}\right]. \quad (3)$$

The porosity of the hybrid was measured to be ~0.5 (i.e. $f = 0.5$), then ε_{eff} for the solvent-saturated hybrid is

$$\varepsilon_{\text{eff}} = 4\left[\frac{1 + 0.5(\sqrt{\varepsilon_{\text{solvent}}/4} - 1)}{1 + 0.5\sqrt{4/\varepsilon_{\text{solvent}}} - 1}\right]. \quad (4)$$

By modifying $\varepsilon_{\text{solvent}}$ with ε_{eff} the correlation between the modified ε_{eff} with spectrum shift (Δ) can be reconstructed, as given in figure 6(a). Following a curve fitting, a best-fitted second-order polynomial equation, with an R^2 as high as 0.9745, can then be obtained, which gives

$$\Delta = 0.361\varepsilon_{\text{eff}}^2 - 3.215\varepsilon_{\text{eff}} + 5.953. \quad (5)$$

Equation (5) is an experimentally derived mathematical model describing the nonlinear relationship between the photoluminescence optical shift and a given effective dielectric environment for the CdS–pHEMA hybrid. Such a nonlinearity also implies the complexity, i.e. a second-order correlation, between the optical structure of the CdS NCs and the surrounding dielectric environment. As a first approximation, the influence of a multi-phase dielectric environment on photoluminescence emission variation is successfully described in this simple model for the hybrids currently developed.

A derivation of Δ in terms of ε_{eff} gives a first-order equation as below:

$$\mathrm{d}\Delta/\mathrm{d}\varepsilon_{\text{eff}} = 0.722\varepsilon_{\text{eff}} - 3.125 \quad (6)$$

which indicates that the ratio of spectrum shift over a unit change of the dielectric constant ($\mathrm{d}\Delta/\mathrm{d}\varepsilon_{\text{eff}}$, termed the 'relative spectrum shift') correlated linearly with the ε_{eff} of the hybrid. Equation (6) reveals an interesting behavior that the change of the relative spectrum shift is linearly increased with increasing effective dielectric constant. This finding strongly suggests that this nanoporous, transparent CdS–pHEMA hybrid can be used as a new type of functional material for a number of practical applications, for instance, chemical sensors. The relative spectrum shift or 'sensitivity' of the hybrid can be proportionally stimulated by its surrounding dielectric environment and equation (6) further suggests that the sensitivity of this hybrid is increased for liquids with high dielectric constant.

In an RH system, the porosity of the hybrid is filled with a mixture of water and air (i.e. an unsaturated condition). The effective dielectric constant is then a combination of pHEMA, water and air. Since Gao's model is accessible only for a two-component system and is hard to apply directly to a current three-component system. For simplicity, the rule of mixtures is applied to estimate the effective dielectric constant of the solvent mixture, i.e. air + water, which is approximated as

$$\varepsilon_{\text{solvent}} = x\varepsilon_{\text{water}} + y\varepsilon_{\text{air}} \quad (7)$$

where

$$x + y = 1. \quad (8)$$

The volume fractions of water (x) under various RHs are given in the inset of figure 6(b). Then the obtained $\varepsilon_{\text{solvent}}$ is employed and the effective dielectric constant of the hybrid under unsaturated condition, ε_{eff}, can be re-estimated using equation (2). Furthermore, we attempt to compare experimental shifts with calculated shifts. The calculated shift is essentially a sum of both the quantum-confinement effect $\Delta E_g^{\text{brus}}(a)$ and dielectric-confinement effect $\Delta E_g^{\text{dielectric}}(a)$ [38–43]:

$$\Delta E_g(a) = \Delta E_g^{\text{brus}}(a) + \Delta E_g^{\text{dielectric}}(a). \quad (9)$$

The size-dependent quantum-confinement energy $\Delta E_g^{\text{brus}}(a)$ can be expressed as

$$\Delta E_g^{\text{brus}}(a) = \frac{\hbar^2\pi^2}{2a^2}\left[\frac{1}{m_e^*} + \frac{1}{m_h^*}\right] - \frac{1.8e^2}{4\pi\varepsilon_0\varepsilon_{\text{CdS}}} \tag{10}$$

where a, ε_0, m_e^* and m_h^* are the radius of the QD, vacuum permittivity, and the effective masses of electrons and holes, respectively. The values of a, ε_{CdS}, m_e^* and m_h^* are 2.2 (nm), 5.4, $0.2m_0$ and $0.8m_0$, respectively.

The dielectric-confinement energy $\Delta E_g^{\text{dielectric}}(a)$ can be expressed as

$$\Delta E_g^{\text{dielectric}}(a) = 2\Delta E_g(a) + \Delta E_c(a) + \Delta E_p(a) \tag{11}$$

where

$$\Delta E_g(a) = \frac{v_s}{a\varepsilon_{\text{CdS}}}. \tag{12}$$

From equation (10)

$$v_s = v_s^0 + \delta v_s. \tag{13}$$

From equation (11)

$$v_s^0 = -\frac{\varepsilon_{\text{CdS}}e^2}{8\pi\varepsilon_0}\left(\frac{1}{\varepsilon_{\text{CdS}}} - \frac{1}{\varepsilon_{\text{eff}}}\right) = -3.88\left(\frac{1}{\varepsilon_{\text{CdS}}} - \frac{1}{\varepsilon_{\text{eff}}}\right) \tag{14}$$

and

$$\delta v_s = 0.27 \tag{15}$$

$$\Delta E_c(a) = \frac{-2.57}{a\varepsilon_{\text{CdS}}} \tag{16}$$

$$\Delta E_p(a) = \frac{e^2}{4\pi a\varepsilon_0\varepsilon_{\text{CdS}}}\left(1 - \frac{\varepsilon_{\text{CdS}}}{\varepsilon_{\text{eff}}}\right). \tag{17}$$

The effective dielectric constant obtained from equation (7) is substituted in equations (14) and (17) to calculate v_s^0 and $\Delta E_p(a)$. The value of $\Delta E_g^{\text{dielectric}}(a)$ can be obtained from equations (12)–(17). The values of the calculated spectrum shift generally higher than that of experimental data in the lower RH region, but become closer to the experimental outcomes as RH increased. Such a discrepancy at lower RH region may be a result of insufficient or uneven distribution of the solvent mixture over all the exposed surface of the CdS QDs in the matrix, rendering the true ε_{eff} of the hybrid much lower than the calculated level. However, as RH increased, the dielectric phase distribution should be more uniformly spread throughout the matrix, giving values reasonably close to those from calculation. However, such a discrepancy may be eliminated for a hybrid with lower dimensions, such as thin film or small particles, in order to enhance its accuracy and sensitivity in sensing the change in the dielectric environment.

Considering the potential use of such a novel hybrid as an opto-chemical sensor for solvents or molecules with varying degrees of dielectric properties, the function of selectivity for a specific dielectric liquid or molecule turns out to be important; however, it has not yet been verified in the current investigation. It is generally a guideline from experimental outcomes that liquids or molecules with lower dielectric constants cause a smaller optical shift of the photoluminescence emission spectrum of the hybrid and, vice versa, a larger spectrum shift occurs for higher dielectric liquids or molecules. However, the issue to enhance further the 'sensibility' of the hybrid to small amounts of dielectric liquid is interesting and will be an important objective of further work.

4. Conclusions

A nanoporous, transparent CdS–pHEMA hybrid with highly uniformly dispersed CdS nanoparticles over the size range of 3–5 nm in diameter was successfully synthesized. Trace amounts, about 4 vol%, of the CdS NCs uniformly embedded in the hybrid permits high accessibility and sensitivity for various dielectric liquids, where a dielectric-confinement effect has been stimulated as a result of the optical shift of the photoluminescence emission spectrum in the presence of dielectric liquids. The effective dielectric constant of the dielectric environment (a mixture of pHEMA, air and solvent) of the hybrid and the resulting mathematical model for predicting the photoluminescence emission shift has been experimentally derived, and has been found to be sensitive to environmental stimuli, i.e. varying the dielectric environment. Sensitivity of the hybrid to the presence of dielectric liquids, even in fractional amounts, has been largely enhanced due to a combination of highly uniformly distributed CdS NCs, even in trace amounts, with a nanoporous pHEMA matrix. It is envisioned that this novel hybrid can be used as a functional material for chemical sensing applications via a change in its optical appearance and/or photoluminescence emission spectra as a result of dielectric stimulus.

References

[1] Alivisatos A P 1996 *Science* **271** 933
[2] Klimov V L, Mikhailovsky A A, Xu S, Malko A, Hollingsworth J A, Leatherdale C A, Eisler H J and Bawendi M G 2000 *Science* **290** 314
[3] Peng X G, Manna L, Yang W D, Wickham J, Scher E, Kadavanich A and Alivisatos A P 2000 *Nature* **404** 59
[4] Chaudhary S, Ozkan M and Chan W C 2004 *Appl. Phys. Lett.* **84** 2925
[5] Coe S, Woo W K, Bawendi M and Bulovic V 2002 *Nature* **420** 800
[6] Ballou B, Lagerholm B C, Ernst L A, Bruchez M P and Waggoner A S 2004 *Bioconjug. Chem.* **15** 79
[7] Dubertret B, Skourides P, Norris D J, Noireaux V, Brivanlou A H and Libchaber A 2002 *Science* **298** 1759
[8] Wu X Y, Liu H J, Liu J Q, Haley K N, Treadway J A, Larson J P, Ge N F, Peale F and Bruchez M P 2003 *Nat. Biotechnol.* **21** 41
[9] Peng X G and Xiao M 2003 *Nano Lett.* **3** 819
[10] Ellis A B 2000 *Macromolecules* **33** 582
[11] Liz-Marzán L M and Mulvaney P 2003 *J. Phys. Chem.* B **107** 7312
[12] Xu S, Zhang J, Paquet C, Lin Y and Kumacheva E 2003 *Adv. Funct. Mater.* **13** 468
[13] Lee J, Sundar V C, Heine J R, Bawendi M G and Jensen K F 2000 *Adv. Mater.* **12** 1102
[14] Zhang H, Cui Z, Wang Y, Zhang K, Ji X, Lu C, Yang B and Gao M 2003 *Adv. Mater.* **15** 777
[15] Farmer S C and Patten T E 2001 *Chem. Mater.* **13** 3920

[16] Gaponik N, Talapin D V, Rogach A L, Eychmuller A and Weller H 2002 *Nano Lett.* **2** 803
[17] Moffitt M, Vali H and Eisenberg A 1998 *Chem. Mater.* **10** 1021
[18] Pavel F M and Mackay R A 2000 *Langmuir* **16** 8568
[19] Chew C H, Li T D, Gan L H, Quek C H and Gan L M 1998 *Langmuir* **14** 6068
[20] Brust M, Walker M, Bethell D, Schiffrin D J and Whyman R 1994 *J. Chem. Soc. Chem. Commun.* 801
[21] Li C L and Murase N 2004 *Langmuir* **20** 1
[22] Zhang H, Cui Z, Wang Y, Zhang K, Ji X, Lu C, Yang B and Gao M 2003 *Adv. Mater.* **15** 777
[23] Kroll E, Winnik F M and Ziolo R F 1996 *Chem. Mater.* **8** 1594
[24] Kane R S, Cohen R E and Silley R 1999 *Chem. Mater.* **11** 90
[25] Dai J and Bruening M L 2002 *Nano Lett.* **2** 497
[26] Wang T C, Rubner M F and Cohen R E 2002 *Langmuir* **18** 3370
[27] Sun Z B, Chen W Q, Dong X Z and Duan X M 2007 *Chem. Lett.* **36** 156
[28] Ranucci E, Ferruti P, Opelli P, Ferrari V, Marioli D and Taroni A 1994 *Sensors Mater.* **5** 221
[29] Luccio T D, Laera A M and Tapfer L 2006 *J. Phys. Chem.* B **110** 12603
[30] Moffitt M, Vali H and Eisenberg A 1998 *Chem. Mater.* **10** 1021
[31] Spanhel L, Haase M, Weller H and Henglein A 1987 *J. Am. Chem. Soc.* **109** 5649
[32] Liu Y Y, Tung T H, Li T Y, Chen S Y and Liu D M 2008 *Acta Biomater.* **4** 2052
[33] Zhao P Q, Wu X L, Fan J Y, Paul K C and Siu G G 2006 *Scr. Mater.* **55** 1123
[34] Tsu R and Babić D 1994 *Appl. Phys. Lett.* **64** 1806
[35] Franceschetti A and Zunger A 2000 *Phys. Rev.* B **62** 2614
[36] Zahn M, Oohi Y, Fenneman D B, Gripshover R J and Gehman V H 1986 *Proc. IEEE* **74** 1182
[37] Gao L and Gu J Z 2002 *J. Phys. D: Appl. Phys.* **35** 267
[38] Brus L E 1983 *J. Chem. Phys.* **79** 5566
[39] Babić D, Tsu R and Greene R F 1992 *Phys. Rev.* B **45** 14150
[40] Iwamatsu M, Fujiwara M, Happo N and Horii K 1997 *J. Phys.: Condens. Matter* **9** 9881
[41] Allan G, Delerue C, Lannoo M and Martin E 1995 *Phys. Rev.* B **52** 11982
[42] Das S, Chakrabarti S and Chaudhuri S 2005 *J. Phys. D: Appl. Phys.* **38** 4021
[43] Lannoo M, Delerue C and Allan G 1995 *Phys. Rev. Lett.* **74** 3415